

AD-A095 753

STANFORD UNIV CA  
A NEW FAMILY OF CAPILLARY WAVES, (U)  
APR 79 J B KELLER, J VANDEN-BROECK

F/G 20/4

DAAG29-79-C-0222

UNCLASSIFIED

ARO-16997.14-M

NL

1 of 1  
40  
2000-7-3



END  
DATE  
FILED  
3 81  
DTIC

UNCLASSIFIED

SECURITY CLASSIFICATION OF THIS PAGE (When Data Entered)

2

<b>19</b> REPORT DOCUMENTATION PAGE		READ INSTRUCTIONS BEFORE COMPLETING FORM
1. REPORT NUMBER 16997.14-M (DARK)	2. GOVT ACCESSION NO. N/A AD-A093753	3. RECIPIENT'S CATALOG NUMBER N/A
4. TITLE (and Subtitle) A New Family of Capillary Waves	5. TYPE OF REPORT & PERIOD COVERED REPRINT	
7. AUTHOR(s) Joseph B. Keller J. - / - / Vandenbroeck	6. PERFORMING ORG. REPORT NUMBER N/A	8. CONTRACT OR GRANT NUMBER(s) DAAG29-79-C-0222 ✓
9. PERFORMING ORGANIZATION NAME AND ADDRESS Stanford University Stanford, CA 94305	10. PROGRAM ELEMENT, PROJECT, TASK AREA & WORK UNIT NUMBERS N/A	
11. CONTROLLING OFFICE NAME AND ADDRESS US Army Research Office PO Box 12211 Research Triangle Park, NC 27709	12. REPORT DATE 1980	13. NUMBER OF PAGES 9 (1) 10
14. MONITORING AGENCY NAME & ADDRESS (if different from Controlling Office)	15. SECURITY CLASS. (of this report) Unclassified	15a. DECLASSIFICATION/DOWNGRADING SCHEDULE
16. DISTRIBUTION STATEMENT (of this Report) Submitted for announcement only		
17. DISTRIBUTION STATEMENT (of the abstract entered in Block 20, if different from Report) DTIC SELECTED FEB 27 1981 B		
18. SUPPLEMENTARY NOTES		
19. KEY WORDS (Continue on reverse side if necessary and identify by block number)		
20. ABSTRACT (Continue on reverse side if necessary and identify by block number)		

AD A 093753

DTIC FILE COPY

334550

sh

ARO 16997.14M

## A new family of capillary waves

By JEAN-MARC VANDEN-BROECK† AND  
 JOSEPH B. KELLER‡

Courant Institute of Mathematical Sciences, New York University,  
 251 Mercer Street, New York, NY 10012

(Received 5 April 1979)

A new family of finite-amplitude periodic progressive capillary waves is presented. They occur on the surface of a fluid of infinite depth in the absence of gravity. Each pair of adjacent waves touch at one point and enclose a bubble at pressure  $P$ .  $P$  depends upon the wave steepness  $s$ , which is the vertical distance from trough to crest divided by the wavelength. Previously Crapper found a family of waves without bubbles for  $0 \leq s \leq s^* = 0.730$ . Our solutions occur for all  $s > s^{**} = 0.663$ , with the trough taken to be the bottom of the bubble. As  $s \rightarrow \infty$ , the bubbles become long and narrow, while the top surface tends to a periodic array of semicircles in contact with one another. The solutions were obtained by formulating the problem as a nonlinear integral equation for the free surface. By introducing a mesh and difference method, we converted this equation into a finite set of nonlinear algebraic equations. These equations were solved by Newton's method. Graphs and tables of the results are included. These waves enlarge the class of phenomena which can occur in an ideal fluid, but they do not seem to have been observed.

### 1. Introduction

Crapper (1957) found a one-parameter family of explicit exact solutions for two-dimensional periodic progressive capillary waves of finite amplitude in water of infinite depth. The parameter is the steepness  $s$ , which is the vertical distance from trough to crest divided by the wavelength. His solutions are valid from  $s = 0$ , when the surface is flat, to  $s = s^* = 0.730$ , when each two adjacent waves touch one another at one point (see figure 1). For  $s > s^*$ , his formulae yield overlapping waves with multiple-valued velocities, so they are not admissible as solutions of the physical problem. Thus the wave of greatest steepness in this family is that with  $s = s^*$ .

We have found a new family of waves of still greater steepness. They all have adjacent waves touching at one point, just like Crapper's highest wave. Thus each two adjacent waves enclose a region devoid of fluid, which we call a bubble. The pressure  $P(s)$  in the bubble is an increasing function of the steepness, with  $P = 0$  at  $s = s^*$  (see figure 2). These waves exist for all  $s > s^{**} = 0.663$ , with  $P(s)$  tending to a constant as  $s$  tends to  $+\infty$ . Thus, in the interval  $s^{**} < s < s^*$ , both these waves and those found by Crapper exist, while, for  $s > s^*$ , the new waves exist while Crapper's do not. Some typical profiles of the waves and bubbles are shown in figure 3.

† Present address: Department of Mathematics, Stanford University, CA 94305.

‡ Present address: Department of Mathematics and Mechanical Engineering, Stanford University, California 94305.

Our investigation was suggested by the work of Flaherty, Keller & Rubinow (1972) on post-buckling behaviour of elastic tubes and rings with opposite sides in contact, and by that of Flaherty & Keller (1973) on contact problems involving a buckled elastica. The method of solution is numerical, based upon the formulation of the problem as an integral equation for the free surface, as in Schwartz & Vanden-Broeck (1979) and Vanden-Broeck & Schwartz (1979).

Kinnersley (1976) extended Crapper's exact result to fluids of finite depth. His highest wave also occurred when adjacent waves touched. Schwartz & Vanden-Broeck (1979) computed numerically capillary-gravity waves in water of infinite depth. In all the cases they considered the solutions were limited by contact of adjacent waves. The present method could be used to extend their solutions, as well as Kinnersley's, to greater values of the steepness.

## 2. Formulation and solution without bubbles

Let us consider two-dimensional periodic capillary waves on the surface of an infinitely deep fluid. We assume that they are symmetric, have wavelength  $\lambda$ , and propagate with phase velocity  $c$  without change of shape. Then we choose a reference frame in which the waves are steady, as is the fluid motion, which is assumed to be a potential flow. We also measure lengths in units of  $\lambda$  and velocities in units of  $c$ , so that all variables become dimensionless. Then we introduce rectangular co-ordinates  $(x, y)$  with the origin at a crest, with the  $x$  axis parallel to the velocity at infinite depth and with the  $y$  axis directed out of the fluid.

The fluid flow can be described by giving  $z = x + iy$  as an analytic function of the complex potential  $f = \phi + i\psi$  in the region  $\psi \leq 0$ . We choose the stream function  $\psi$  to vanish on the free surface, and we set  $\phi = 0$  at  $x = y = 0$ . Then the free surface is given parametrically by  $x(\phi, 0)$ ,  $y(\phi, 0)$ , which we shall write as  $x(\phi)$ ,  $y(\phi)$ . We denote the complex velocity by  $q = u - iv$ , and by our choice of variables  $u$  tends to 1 and  $v$  tends to zero as  $\psi$  tends to  $-\infty$ .

Now the dynamical condition at the free surface yields the Bernoulli equation

$$q\bar{q} - 1 + T\kappa = 0 \quad \text{on} \quad \psi = 0. \quad (2.1)$$

Here  $\bar{q}$  is the complex conjugate of  $q$ ,  $\kappa(\phi)$  is the curvature of the free surface (counted positive when the centre of curvature is on the fluid side of the surface) and  $T$  is the dimensionless parameter

$$T = 2\sigma/\rho\lambda c^2. \quad (2.2)$$

In (2.2)  $\rho$  is the fluid density and  $\sigma$  is the surface tension of the surface. The choice of the constant in (2.1) implies that the pressure above the surface equals that at infinite depth. Without loss of generality, we can set these pressures equal to zero.

To determine the free surface we note that the function  $x_\phi + iy_\phi - 1$  is analytic in the half-plane  $\psi \leq 0$  and vanishes at  $\psi = -\infty$ . Therefore its imaginary part on the line  $\psi = 0$  is the Hilbert transform of its real part:

$$y_\phi(\phi) = \frac{1}{\pi} \int_{-\infty}^{\infty} \frac{x_\phi(\phi') - 1}{\phi' - \phi} d\phi'. \quad (2.3)$$

The integral in (2.3) is to be understood in the Cauchy principal value sense.

We now use the assumed periodicity and symmetry of the surface to rewrite (2.3) in the form

$$y_\phi(\phi) = \int_0^{\frac{1}{2}} [x_\phi(\phi') - 1] [\cot \pi(\phi' - \phi) - \cot \pi(\phi' + \phi)] d\phi'. \quad (2.4)$$

We next rewrite the condition (2.1) as

$$(x_\phi^2 + y_\phi^2)^{-1} - 1 - T(x_\phi y_{\phi\phi} - y_\phi x_{\phi\phi}) (x_\phi^2 + y_\phi^2)^{-\frac{3}{2}} = 0. \quad (2.5)$$

Finally we note that the steepness  $s$  of the waves can be expressed in terms of  $y_\phi(\phi)$  by the formula

$$s = - \int_0^{\frac{1}{2}} y_\phi(\phi) d\phi. \quad (2.6)$$

For a given value of  $s$ , (2.4)–(2.6) are a set of integro-differential equations for the functions  $x_\phi(\phi)$ ,  $y_\phi(\phi)$  and the parameter  $T$ . The surface shape  $x(\phi)$ ,  $y(\phi)$  can be obtained from the solution by integration, and the wave speed  $c$  can be found from (2.2). The solution of these equations should be Crapper's solution.

To solve these equations, we introduce the  $N + 1$  mesh points  $\phi_i = (i - 1)/2N$  and the unknowns  $x'_i = x_\phi(\phi_i)$ ,  $i = 1, \dots, N + 1$ . Then we compute  $y'_{i+\frac{1}{2}}$  midway between mesh points from (2.4) using the trapezoidal rule. Next we compute  $y'_i$  and  $y'_i$  from the  $y'_{i+\frac{1}{2}}$  by a centred four-point Lagrange interpolation formula and a centred four-point difference formula, respectively, using the periodicity and symmetry of  $x_\phi$ . We also compute  $x'_i$  from the  $x'_i$  by a four-point difference formula. By using these expressions in (2.5) at the points  $\phi_i$ , we obtain a system of  $N + 1$  nonlinear algebraic equations. Then by using (2.4) in (2.6) we obtain another algebraic equation. Thus we obtain  $N + 2$  equations for the  $N + 2$  unknowns  $x'_1, \dots, x'_{N+1}, T$ . We solve these equations by Newton's method. The entire numerical procedure follows closely that used by Vanden-Broeck & Schwartz (1979) and Schwartz & Vanden-Broeck (1979).

Some of the results obtained by this method for  $0 \leq s \leq s^*$  are shown in table 1 and in figure 1. They were obtained for various values of  $s$  with  $N = 40$  and  $N = 60$ . The results for these two values of  $N$ , shown in table 1, agree to four decimal places. They also agree well with Crapper's exact solution, which is given in the last column of the table. This is a good check on our numerical method.

In figure 1, a few free surface profiles are shown for different values of  $s$  up to  $s = 0.73$ , at which the surface touches itself and forms a bubble. For  $s > 0.73$  our numerical solution crosses itself, just as does Crapper's exact solution. Then the solution is not physically meaningful. In Crapper's solution, the streamlines of the flow for a wave of given steepness are themselves free surface profiles for waves of smaller steepness, so they are shown that way in figure 1.

### 3. Waves with bubbles

To obtain solutions for  $s \geq s^*$  we require the free surface to be in contact with itself at one point within each wavelength. Let us denote by  $\alpha$  the  $\phi$  co-ordinate of the contact point in the interval  $0 \leq \phi \leq \frac{1}{2}$ . Then by symmetry we have

$$x_\phi(\alpha) = 0, \quad (3.1)$$

$$x(\alpha) = \int_0^\alpha x_\phi(\phi') d\phi' = \frac{1}{2}. \quad (3.2)$$

If we adjoin (3.1) and (3.2) to (2.4)–(2.6), we have two additional equations but only

tion	<input checked="" type="checkbox"/>
ion	<input type="checkbox"/>
	<input type="checkbox"/>
CODES	
SPECIAL	

6-2  
A 20/21

$s$	$N = 40$	$N = 60$	Crapper
0.1	0.32221	0.32221	0.32221
0.2	0.33365	0.33365	0.33365
0.3	0.35188	0.35188	0.35188
0.5	0.40474	0.40475	0.40475
0.73	0.48428	0.48430	0.48430

TABLE 1. Comparison of computed values of  $T$  for  $N = 40$  and  $N = 60$  with Crapper's exact value.

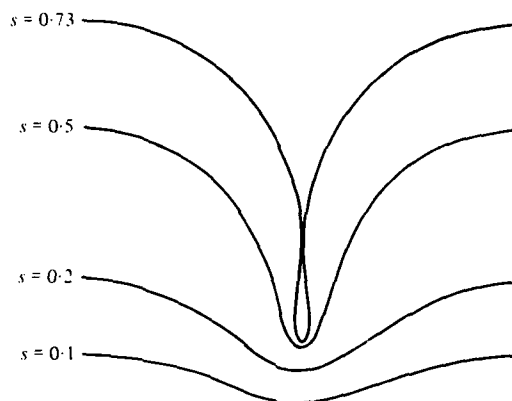


FIGURE 1. Computed free surface profiles for various values of the steepness  $s$ . The unit of length is the wavelength. These results agree with Crapper's explicit solution for  $0 \leq s \leq 0.73$ .

one additional unknown,  $\alpha$ . Therefore we cannot expect the enlarged set of equations to have a solution for any value of  $s$  other than  $s^*$ , when the solution is Crapper's highest wave, which satisfies (3.1) and (3.2) with  $\alpha = \alpha^* = 0.17$ . This expectation is in agreement with the results of numerical calculation which did yield Crapper's solution for  $s = s^*$ , but which did not yield any solution for  $s > s^*$ .

The physical reason why the enlarged problem does not have a solution with  $s > s^*$  is that it requires the pressure  $P$  in the bubble to be the same as that above the free surface, i.e. to be  $P = 0$ . It is to be expected that the pressure within a bubble will have some value other than zero, which we cannot prescribe. Therefore we shall modify the free surface condition (2.5) by introducing the unknown bubble pressure  $P$  into it in the interval  $\alpha < \phi \leq \frac{1}{2}$ , which corresponds to the bubble surface. Thus we replace (2.5) by

$$(x_\phi^2 + y_\phi^2)^{-1} - 1 - T(x_\phi y_{\phi\phi} - y_\phi x_{\phi\phi})(x_\phi^2 + y_\phi^2)^{-\frac{3}{2}} = \begin{cases} 0, & 0 \leq \phi < \alpha, \\ -P, & \alpha < \phi \leq \frac{1}{2}. \end{cases} \quad (3.3)$$

Here  $P$  is measured in units of  $\rho c^2$ .

Now we consider (2.4), (2.6), (3.1)–(3.3) as a set of equations for  $x_\phi(\phi)$ ,  $y_\phi(\phi)$ ,  $T$ ,  $\alpha$  and  $P$ , for a given value of  $s$ . We have added the two equations (3.1) and (3.2) to the problem of §2, and added the two unknowns  $\alpha$  and  $P$ , so we expect the new problem to be solvable.

$s$	$P$	$T$	$K$	$S$
0.6635	-1.6	0.4727	3.11	3.8
0.7	-0.28	0.4801	3.36	4.08
0.73	0	0.4843	3.57	4.31
0.75	0.13	0.4863	3.71	4.46
0.85	0.48	0.4933	4.43	5.24
1.05	0.75	0.4983	5.93	6.83
1.4	0.89	0.4998	8.61	9.66

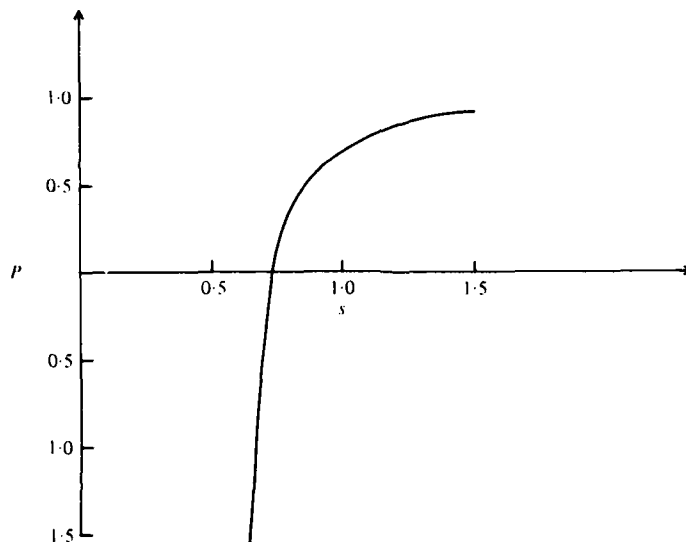
TABLE 2. Computed values of  $P$ ,  $T$ ,  $K$  and  $S$  for various values of  $s$ .

FIGURE 2. The bubble pressure  $P$  (in units of  $\rho c^2$ ) versus the steepness  $s$  for the new family of waves with bubbles.  $P$  tends to unity as  $s \rightarrow \infty$  and  $P = 0$  at  $s = 0.73$ . The axis  $P = 0$  corresponds to Crapper's solution, which is physically meaningful for  $0 \leq s \leq 0.73$  and unphysical for  $s > 0.73$ .

We shall solve this problem by a numerical method similar to that of the previous section. We introduce the  $N_1 + N_2 + 1$  mesh points  $\phi_i$  defined by

$$\left. \begin{aligned} \phi_i &= \alpha(i-1)/N_1, & i &= 1, \dots, N_1, \\ \phi_i &= \alpha + (\frac{1}{2} - \alpha)(i - N_1 - 1)/N_2, & i &= N_1 + 1, \dots, N_1 + N_2 + 1. \end{aligned} \right\} \quad (3.4)$$

We then introduce the corresponding unknowns  $x'_i = x'_\phi(\phi_i)$ . Next we discretize (2.4) and (2.5) at the mesh points. In doing so, we observe from (3.3) that the curvature of the surface jumps by  $-P/T$  at  $\phi = \phi_{N_1+1} = \alpha$ . Therefore, in interpolating and finite differencing at a point on either side of this discontinuity, we use only mesh points on the same side.

By using the differenced form of (2.4) as before to eliminate  $y_\phi$  from the differenced form of (2.5), we obtain a set of  $N_1 + N_2 + 1$  nonlinear algebraic equations for the  $N_1 + N_2 + 4$  unknowns  $x'_i$ ,  $T$ ,  $\alpha$  and  $P$ . We get three more equations from (2.6), (3.1) and (3.2), thus obtaining  $N_1 + N_2 + 4$  equations for the same number of unknowns. This system of equations is solved by Newton's method.

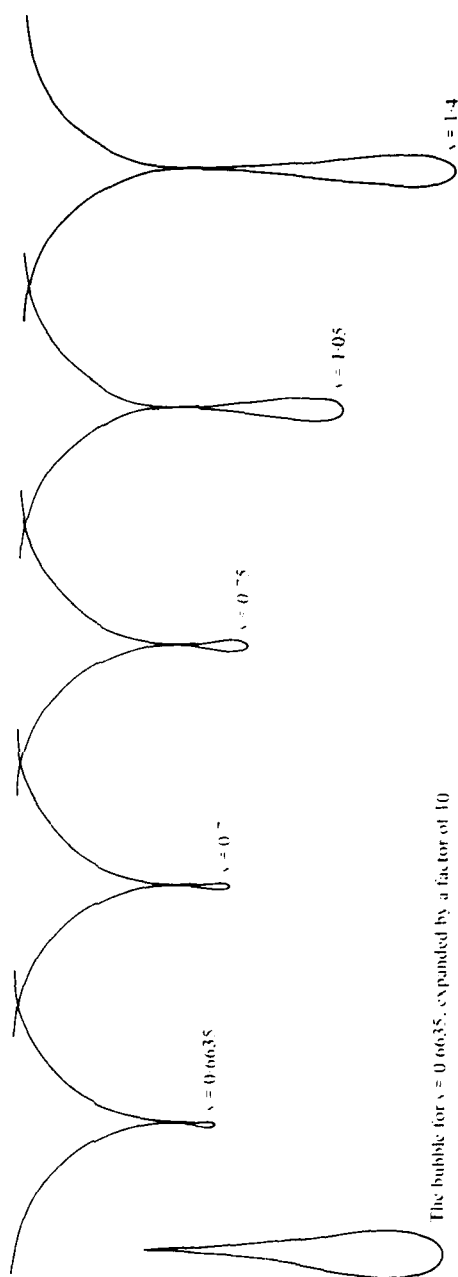


FIGURE 3. Computed profiles of the free surface and bubble for five values of  $s$ .

For  $s$  slightly greater than  $s^*$ , the iterations are started with Crapper's highest wave as a first approximation. After the iterations converge, the solution is used as an initial approximation to compute the solution for a slightly larger value of  $s$ , and so on. The program was run on a CDC 6600 computer with 60 mesh points.

#### 4. Discussion of results

Our main numerical results are presented in table 2 and in figures 2-5. The bubble pressure  $P$ , computed for various values of the steepness  $s$ , was used to draw the smooth curve in figure 2. This curve crosses the  $s$  axis at  $s = 0.730$ , where  $P = 0$ , and the corresponding solution is Crapper's highest wave. His solution for waves of smaller steepness is represented by the segment of the  $s$  axis from  $s = 0$  to  $s = 0.730$ . The portion of the  $s$  axis with  $s > 0.730$  represents the non-physical analytic continuation of his solution, while the curve represents the physical continuation. Figure 3 gives the computed free surface profiles for various values of  $s$ , and shows that the bubble size increases as  $s$  increases.

We see that the new solution exists both for  $s > 0.730$ , where it is steeper than Crapper's steepest wave, and for  $0.663 < s < 0.730$ . Thus there are two physically admissible solutions for  $0.663 < s < 0.730$ , Crapper's solution and the new one. The pressure  $P$  increases with  $s$  along the curve in figure 2, so the bubble pressure exceeds the (atmospheric) pressure above the fluid for  $s > s^*$  and is less than that pressure for  $s < s^*$ . The largest value of  $s$  for which we have computed the solution is  $s = 1.5$ . We believe that we could compute the solution for larger values of  $s$  by increasing the number of mesh points, and that the solution exists for all  $s > 0.663$ .

As  $s$  increases, the fluid velocity  $q$  at and near the surface decreases to zero as  $s \rightarrow \infty$ . It then follows from (3.3) that the curvature of the free surface tends to the constant value  $-T^{-1}$  for  $0 \leq \phi < \alpha$ . Consequently this portion of the free surface tends to a quarter of a circle, the diameter of which must be equal to the wavelength 1. Therefore its curvature tends to  $-2$ , so  $T$  tends to  $\frac{1}{2}$ . The curvature of the bubble, on the other hand, tends to zero at  $\phi = \alpha$ , and therefore from (3.3) the pressure  $P$  tends to 1.

These considerations indicate that, as  $s \rightarrow \infty$ , the surface tends to a periodic array of semicircles in contact with one another, the bubble boundaries tend to the two sides of the vertical lines beneath the contact points, and the fluid velocity at and near the surface tends to zero. This represents the inner asymptotic form of the solution as  $s \rightarrow \infty$ , for  $y$  fixed.

The outer asymptotic form is represented by the flow beneath a periodic array of bubbles, each of which extends upward to  $y = +\infty$  with a width which tends to zero as  $y \rightarrow +\infty$ . Matching of the two asymptotic solutions shows that the velocity  $q$  in the inner solution is proportional to  $e^{-\pi s}$ , which decreases rapidly as  $s$  increases. The bubble width is also proportional to  $e^{2\pi(y-s)}$ .

The bubbles become very long as  $s$  increases, but adjacent bubbles cannot come into contact with one another. If they did, they and the free surface would enclose a bounded region of fluid which would therefore have to be at rest. Then the adjacent bubble surfaces would be circular arcs concave upward. They cannot be tangent to one another without being semicircles, which would require infinite curvature at the point of tangency. This is not allowed by the free surface condition.

As the steepness  $s$  decreases below 0.730,  $P$  becomes more and more negative and the

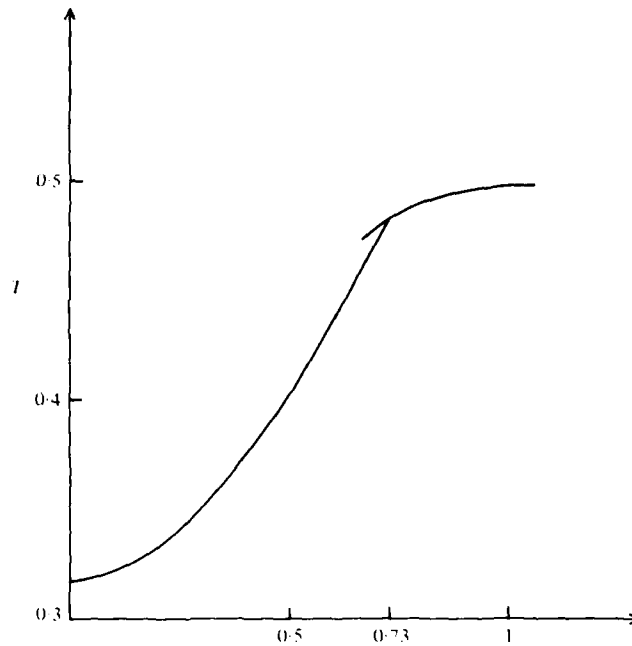


FIGURE 4. The dimensionless parameter  $T = 2\sigma/\rho\lambda c^3$  as a function of the steepness  $s$ . The lower curve corresponds to Crapper's solution and the upper curve to the new solution. These curves determine the wave velocity  $c$  in terms of  $\lambda$  and  $s$ , so they represent the nonlinear dispersion equation for the waves.

bubble becomes smaller. Figure 3 shows that the curvature at  $\phi = \alpha_-$  is positive. Thus the bubble cannot shrink to a point as  $s$  decreases. If it did the velocity at  $\phi = \alpha_-$  would tend to infinity. Then the curvature at  $\phi = \alpha_-$  would have to be negative in order to satisfy (3.3).

We conclude that the smallest steepness  $s^{**}$  for which our family exists corresponds to zero curvature at  $\phi = \alpha_-$ . We found numerically that  $s^{**} = 0.663$ . As we expected, the numerical scheme failed to converge for  $s < s^{**}$ .

In figure 4 we present the values of the parameter  $T$  versus the steepness  $s$  for both Crapper's solution and our new family. The two curves cross at  $s = 0.730$ . We note that  $T$  tends to 0.5 as  $s \rightarrow \infty$ . This is in agreement with the asymptotic form of the solution as  $s \rightarrow \infty$ , which is described above.

The kinetic energy  $K$  and the surface energy  $S$  can be computed from our numerical solutions. Following Longuet-Higgins (1975) and Schwartz & Vanden-Broeck (1979), we define  $K$  and  $S$  by the relations

$$K = -\frac{4}{T^2} \int_0^{\frac{1}{2}} y d\phi + \frac{4}{T^2} \int_0^{\frac{1}{2}} y x' d\phi, \quad (4.1)$$

$$S = \frac{2}{T} \left[ 2 \int_0^{\frac{1}{2}} (x'^2 + y'^2)^{\frac{1}{2}} d\phi - 1 \right]. \quad (4.2)$$

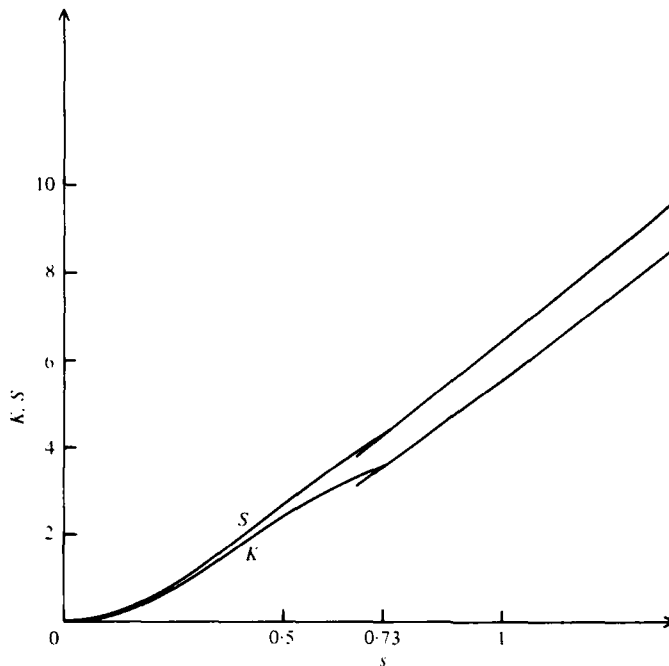


FIGURE 5. The kinetic energy  $K$  and the surface energy  $S$ , per wavelength (in units of  $\sigma^2/\rho c^2$ ) as functions of the steepness  $s$ . The lower portion of each curve corresponds to Crapper's solution, and the upper portion to the new solution. The upper portions are very nearly straight lines.

The integrals in (4.1) and (4.2) were computed by the trapezoidal rule. Figure 5 shows the kinetic energy  $K$  and the surface energy  $S$  versus the steepness  $s$  for Crapper's family of solutions and for our new family of solutions.

Supported by the Office of Naval Research, the Army Research Office, the Air Force Office of Scientific Research and the National Science Foundation. The numerical calculations were done at the Computing Center of the Courant Institute of Mathematical Sciences, New York University.

#### REFERENCES

- CRAPPER, D. G. 1957 *J. Fluid Mech.* **2**, 532.  
 FLAHERTY, J. E. & KELLER, J. B. 1973 *SIAM J. Appl. Math.* **24**, 215.  
 FLAHERTY, J. E., KELLER, J. B. & RUBINOW, S. I. 1972 *SIAM J. Appl. Math.* **23**, 446.  
 KINNERSLEY, W. 1976 *J. Fluid Mech.* **77**, 229.  
 LONGUET-HIGGINS, M. S. 1975 *Proc. Roy. Soc. A* **342**, 157.  
 SCHWARTZ, L. W. & VANDEN-BROECK, J.-M. 1979 *J. Fluid Mech.* **95**, 119.  
 VANDEN-BROECK, J.-M. & SCHWARTZ, L. W. 1979. *Phys. Fluids* **22**, 1868.

**MED**  
**8**